Fine Guidance Sensor for High-Precision Control of the OAO

NORMAN A. GUNDERSEN*
Sylvania Electronic Systems, Waltham, Mass.

The fine guidance sensor designed for the Princeton Experiment Package of the Orbiting Astronomical Observatory is described. The sensor is capable of providing two axis error signals over a field of view of 4 arc min and with an accuracy of 0.1 arc sec. The sensor uses the light-gathering capability of the experiment's primary optical system and also has its own optical system and electronics system for signal processing. The optical system and electronics block diagram are discussed in detail. Transfer characteristics are described for each axis. The signal-to-noise ratio of the sensor is derived and presented for various star intensities. The effect of several stars in the field of view is described. The redundancy configuration is described, and the predicted reliability is discussed.

THE Orbiting Astronomical Observatory Program was initiated to permit astronomical observations to be made from above the earth's atmosphere. A concept using a standardized spacecraft has been established, and experiments have been planned for studying ultraviolet and infrared radiant energy with varying degrees of precision.

The fourth in the series of experiments is the Princeton Experiment. The main purpose of the Princeton Experiment is to examine the extremely fine absorption lines that we expect to observe when examining the radiation from selected stars. The fine absorption lines are caused by the interstellar gas clouds which exist at extremely low pressure and lie in the line of sight to the star. Figure 1 shows an artist's concept of the spacecraft in orbit. The experiment will be carried on board in a central cylindrical tube which contains the experiment optics plus two bays which contain the experiment electronics.[3]

The experiment will contain a Cassegrain telescope with an 80-cm-diam primary mirror and a high-resolution spectrometer. The requirement for the high-resolution spectrometer arises from the need to examine extremely fine absorption lines. The arrangement of the telescope and spectrometer is shown in Fig. 2. The incoming starlight is collected by the primary mirror where it is then reflected and directed at the secondary mirror, which reflects and focuses the light on the slit jaws of the spectrometer. The slit jaws lie approximately midway between the primary and secondary mirrors. It is expected that the stellar image on the slit jaws will be approximately 50 μ in diameter. The slit jaws have a 24-μ spacing which corresponds to approximately 0.3 arc sec motion of the stellar image in the plane of the slit jaws. Close to 50% of the light energy in the image will fall through the slit, and the balance will fall on the faces of the slit jaws when the image is exactly positioned on the entrance slit of the spectrometer. The light that falls through the slit jaws will be used for spectrophotographic analysis, and the light which falls on the faces of the slit jaws will be used in the fine guidance sensor.

The optical pickoff and detector portion of the fine guidance sensor for the Princeton Experiment Package will be mounted to the spectrometer housing adjacent to the slit. The electronics for processing the signals will be located within the electronics box. The sensor provides a means for measuring the angular error across the slit width by comparing the relative intensities of light energy falling on each side of the slit jaws.[5] The angular error along the length dimension of the slit is measured by comparing the relative light intensities on either side of an imaginary line perpendicular to the slit length. This line is not physically realized at the slit plane but at a biprism located in the path of the light reflected from the slit jaws. The physical arrangement of the optical pickoff is shown in Fig. 3. This figure contains an illustration of the path followed by a beam α which falls on an outer corner of a slit jaw. It shows the path of a beam β which is exactly centered on the slit jaws, and it also shows the loci of points on each element where a beam reflected from a given quadrant of a slit plane will pass. The $f/20$ beam from the telescope is reflected from the slit jaws A through a field lens B of fused silica which images the star at the focal plane D which is merely a point in space but which is shown as a surface for illustrative purposes. The use of fused silica optics increases the bandwidth of useful light energy transmitted by approximately 50%. The mirror C is used only for changing the direction of the beam.

It is to be noted that the plane of the slit has been tilted at an angle to the entering beam so that the light will be reflected off the main axis of the telescope. Each slit jaw is also tilted by a small angle out of the previously mentioned plane, so that division of the beam location is now made for one of the vehicle control axes. This axis is most critical and one where an error signal must be provided for a control accuracy of at least 0.1 arc sec and with a noise on the error signal not greater than a value equivalent to 0.005 arc sec.[7] This division is emphasized at the focal plane D. By providing for the division of energy at the slit jaws for the control axis, requirements for maintenance of alignment are greatly reduced. Division of the beam for the other control axis is obtained by the use of the biprism E. The biprism is located a short distance from the local plane D where it intercepts the out-of-focus beam. The diameter of the out-of-focus beam, as it falls on the first surface of the prism, determines the angular range over which variation of intensity can be obtained for this control axis. Examination of the insert, which shows an enlarged view of the biprism, will show that a beam of light exactly centered on the slit jaws, which will have been first divided by the slit jaws, will be further divided by the biprism and the emerging beams will be caused to diverge at a greater rate than the entering beam.

After leaving the biprism, the beam then passes through the lens F and the beam splitter G. It is then reflected in turn from the optical chopper H and the diagonal mirror J to the face of the detector K. The lens F is a fused silica lens which

Presented as Preprint 63-211 at the AIAA Summer Meeting, Los Angeles, Calif., June 17–20, 1963; revision received October 18, 1963. The information presented here includes contributions from many people. Program direction and evaluation have been provided by Lyman Spitzer Jr. and John B. Rogerson of Princeton University; the system and electronic contributions were made by K. Arbenz and T. Callahan of Sylvania Electronic Systems; and the optical system contributions were made by R. Noble and H. Hemstreet of the Perkin-Elmer Corporation. This work is being performed under the sponsorship of NASA, Contract NAS 5-1810.

* Technical Manager, Princeton Experiment Program.

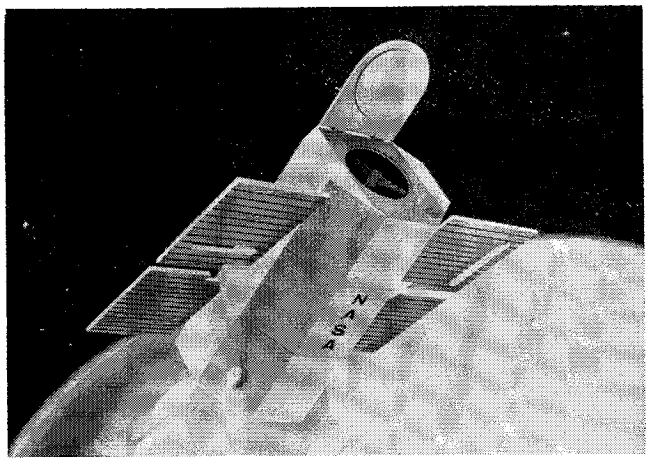

Fig. 1 OAO orbital configuration, artist's concept.

images the focal plane D on the face of the detector K. The beam splitter is also made of fused silica and provides for the splitting of the energy between the redundant detector systems H, J, K, and L, M, N. It transmits 50% of the energy to the chopper H and detector K and reflects the remaining 50% of the light to the chopper L and detector N.

The optical chopper H is an aluminized circular plane mirror with one reflecting sector (slightly less than 90°) and a mask over the remaining sectors. The chopper is fastened to the shaft of a motor with the reflecting surface perpendicular to the axis of the motor. When the motor is operated, the aluminized sector will reflect each quadrant of the slit plane in sequence to the diagonal mirror J and then to the detector K. At any given time, light from only one quadrant will be reflected to the detector face. The position of the light spots in the plane of the reflecting sector of chopper depends only upon which quadrant of the slit plane the star image is located, and not upon its relative position within a particular quadrant. Each quadrant of the slit plane will be reflected to the detector for a length of time equal to the rotation time of the mirror through the sector angle. The output of the detector consists of consecutive sets of four pulses each. The sector angle of the chopper mirror is chosen so that there will be no overlapping of pulses and that there will be a small space between pulses. The amplitude of each pulse is proportional to the area covered by the star image on its corresponding quadrant in the slit plane multiplied by the reflectivity of the area on which it falls. If no light energy appears in a given quadrant then no pulse will appear.

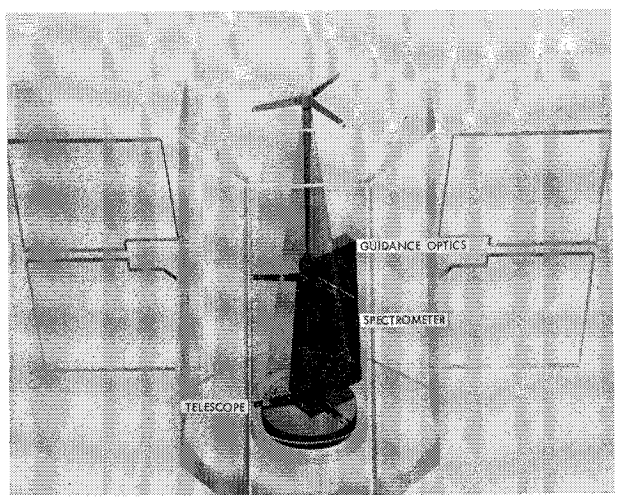

Fig. 2 Phantom view of the OAO showing arrangement of telescope, spectrometer, and guidance optics.

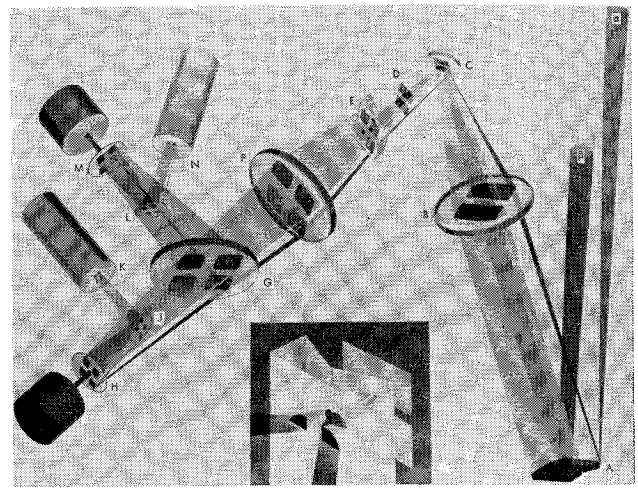

Fig. 3 Optical system of the guidance sensor.

Attached to the chopper motor is a generator which provides the gating signal necessary to separate each pulse from the pulse train and to provide for the proper processing of the pulses. This generator output is also used as a control signal to the motor drive circuit to maintain the motor at nearly constant speed.

From the preceding description, it is seen that the division of light energy into the two paths required for determination of precise guidance is made at the point where such control is required, that is, at the slit jaws. Division at this point greatly reduces the requirements for precision adjustment, and maintenance of alignment of the optical and mechanical parts of the optical pickoff. The detectors are insensitive to image quality and the optical system need not be refocused because of temperature effects.

A block diagram of the electronics is given in Fig. 4. The optical chopper supplies the detector serial information which is then amplified and fed to the gates.

The gate logic provides for the addition of the signals from quadrants 1 and 2, 3 and 4, 1 and 4, and 2 and 3. By inverting 3 + 4 and adding it to 1 + 2, a difference output is obtained which gives the error signal for the axis which is parallel to the slit width. Similarly, inverting 2 + 3 and adding it to 1 + 4, a difference signal is obtained which is the error signal for the axis parallel to the length of the slit.

The output of the detector amplifier is also used for Automatic Gain Control (AGC) purposes. For this purpose, the serial pulses are added to obtain the level of the input signal.

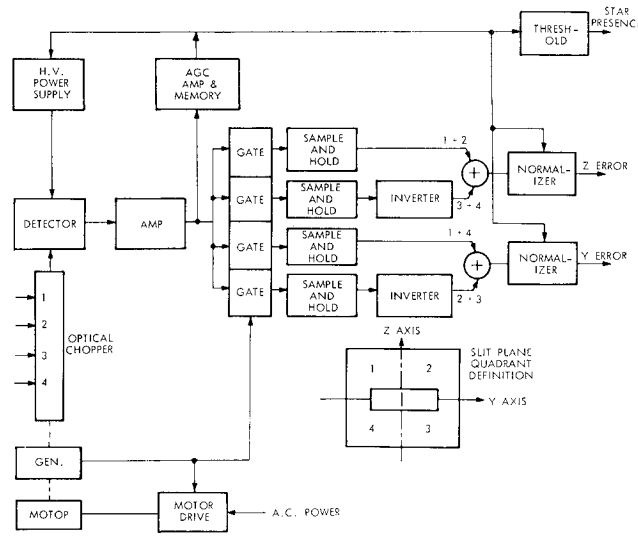

Fig. 4 Guidance sensor electronics block diagram.

This level is then stored in a simple memory circuit. The memory is an r.c. circuit with a given time constant. The output of the AGC amplifier and memory is used to control the anode voltage applied to the detector, a photomultiplier tube. As the signal level increases, the high voltage on the anode string is decreased, and the gain of the tube is decreased. The AGC signal is also used to normalize the error signals as they are processed by the normalizer. This makes the error signals for a given displacement very nearly equal for the range of star magnitudes that are to be observed. The range in star magnitude will be from zero to seventh magnitude and the sensor must provide error signals for maintaining guidance to ± 0.1 arc sec over this range of magnitude. Partial compensation for this dynamic range (approximately 650/1) is accomplished in the photomultiplier gain control. Providing compensation of approximately 100/1 at this point reduces the linear dynamic range requirements to 10/1 for the amplifiers and other electronics which follow. The normalizer provides the remaining 10/1 compensation for an output signal which is independent of star magnitude changes.

Another use of AGC voltage provides a signal to the spacecraft, thus indicating that the fine guidance sensor has a star of seventh magnitude or brighter in its field of view. The level of the AGC signal is measured and compared to a preset threshold value. If the AGC signal exceeds this value, then the threshold circuit provides a voltage level called the "star presence signal" to the spacecraft.

The transfer characteristic that will be provided for the axis parallel to the slit width (the Z axis) is shown in Fig. 5. When the star image has moved by 0.45 arc sec from the center of the slit all the light energy will then be reflected from one slit jaw. This indication would normally give a maximum signal. To provide for a further change in the error signal, the slit jaws are coated so that they reflect only 50% of the light energy at the edge of the slit. The coating is linearly decreased in absorptivity out to 10 arc sec from the center of the slit. The slit jaws have maximum reflectivity at this point and out to the limit of the field (4 arc min).

The time when the spacecraft starts using the error signal from the sensor is called the acquisition mode. During this time the spacecraft may have experienced an initial angular velocity, which must be overcome by the torque limitations and the saturation of the error signal over most of the angular range, the acquisition mode is characterized by an oscillatory motion of the spacecraft about the null position, which is damped only during the ± 10 arc sec interval. When the oscillation has been damped to 10 arc sec amplitude, the slopes of the transfer characteristic provide a much greater damping effect and the spacecraft settles to the null position very rapidly. This is referred to as the fine guidance mode.

During the acquisition mode, the AGC signal has been maintained to maximum value for a given star, since the slit jaws have maximum reflectivity. The memory maintains the AGC level during that part of the swing of the spacecraft when the star signal is attenuated by the coating on the slit jaws, or part of the light enters the slit.

During the fine guidance mode, the reflected star signal amplitude decreases because of the slit jaw coating. The time constant of the memory is about five sec. This maintains the AGC level during the acquisition mode; but when settling on null, the AGC level decays rapidly enough, so that the effect of this time constant on settling time is negligible.

A more detailed analysis of the transfer characteristic will explain the performance of the system more completely.[1] To simplify this analysis, it is assumed that the star image is a uniformly illuminated square whose side is twice the width of the slit. This is shown in Fig. 5. A theoretically ideal model would consider the spot to be the diffraction image of the star whose intensity is a function of its radius from zero to infinity and is given by a Bessel function.

The offset of the image from the null position along the critical Z axis, the axis parallel to the slit width, is measured

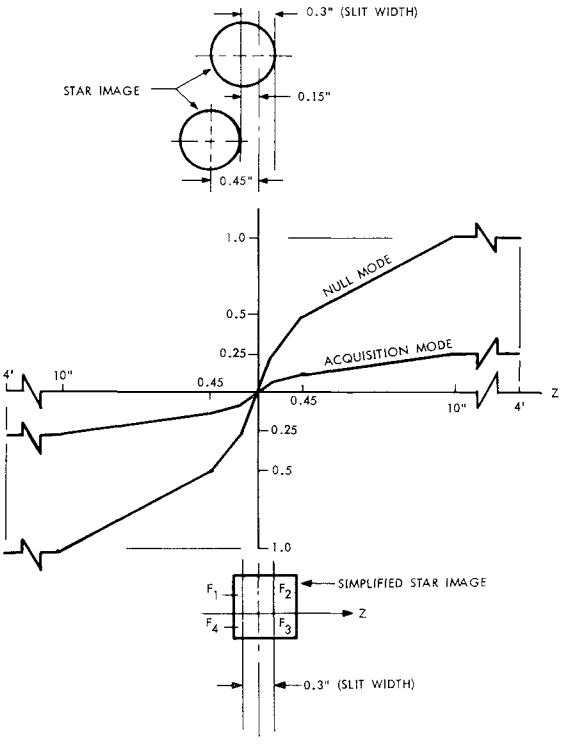

Fig. 5 Transfer characteristic of the Z-control axis.

by comparing the relative light intensities of each part of the image area on either side of the slit. These intensities are proportional to the areas F_1, F_2, F_3, F_4. The normalized difference in intensity defines the error signal and is given by

$$\frac{(F_1 + F_4) - (F_2 + F_3)}{F_1 + F_2 + F_3 + F_4}$$

Since the sum of $F_1 + F_2 + F_3 + F_4$ can vary from 50 to 100% of the total area, depending on whether or not the star image enters the slit, the transfer characteristic may vary between two limiting curves corresponding to 50 and 100% of the image intensity. The transfer characteristic reaches saturation as soon as the square falls completely on one side of the slit, giving a limited range dependent on image size. In order to extend the range, the slit jaws are coated to reduce the reflectivity to 50% at the slit jaw and the reflectivity increases linearly to 100% as the distance from the slit increases. The transfer characteristic will now vary between the two limiting curves corresponding to 25 and 100% of the image intensity because of the addition of this attenuation near null.

The transfer characteristic for the less critical Y direction (parallel to the slit length) is provided in a similar manner by using the out-of-focus image on the biprism. Figure 6 shows the simplified (square) image superimposed on the slit and the biprism edge projected to same plane. If the star image is at the null position, one half of the light passes through each half of the biprism and indicates a zero output for this position. As the star image moves away from the null position, more of the image falls on one half of the biprism than the other and produces a linearly increasing error signal. The linear range of the transfer characteristic will depend upon the size of the image on the biprism. The linear range hf the transfer characteristic can be suitably increased by positioning the biprism slightly away from the plane of focus. The slope of the transfer function will vary between the acquisition mode and the fine guidance mode at null in the same manner as it did for the Z axis.

In order to examine the rms noise error angle of the sensor system, consider the idealized circuit shown in Fig. 7 consisting of a photomultiplier in series with an r.c. filter and polar-

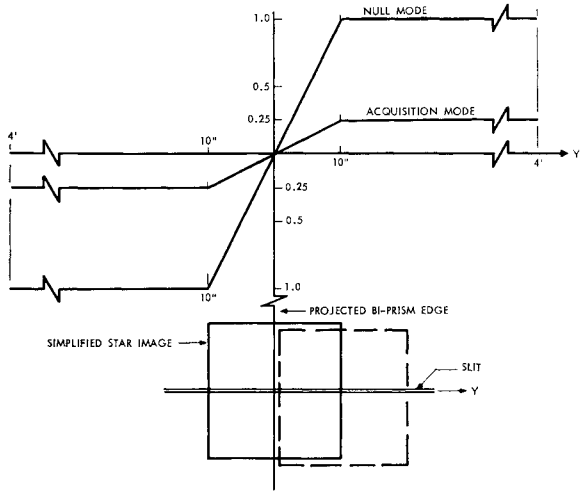

Fig. 6 Transfer characteristic of the Y control axis.

izing battery. The current in the load resistor is amplified by a low-noise preamplifier that has a noise figure of 1 and will not be considered in this analysis.

The noise component of the photomultiplier output current iG is caused not only by the random emission of photoelectrons which results from the random arrival of photons on the photocathode, but also by the thermal emission of electrons from the photocathode. The rms value of the total noise current is given by

$$\overline{(i_n^2)}^{1/2} = [2e(i + i_D)G^2\Delta f]^{1/2} \tag{1}$$

where

e = electron charge
i = average photomultiplier cathode signal current
i_D = cathode dark current (thermal)
Δf = incremental bandwidth
G = photomultiplier gain

An additional source of nonrandom noise is the thermal fluctuation of charge density along the resistor R called Johnson noise. A pure resistance R produces an rms noise voltage:

$$\overline{(V_n^2)}^{1/2} = (4kTR\Delta f)^{1/2} \tag{2}$$

where

k = Boltzmann constant, 1.374×10^{-23} joules/°K
T = °K
R = load resistor, Ω

At room temperature the right-hand side becomes $(0.1eR\Delta f)^{1/2}$. The total rms noise voltage is

$$\overline{(V_n^2)}^{1/2} = \left[2e(i + i_D)G^2 + \frac{4KT}{R}\right]^{1/2}(R^2\Delta f)^{1/2} \tag{3}$$

In Fig. 7 the load resistor is shunted by a capacitor C. The

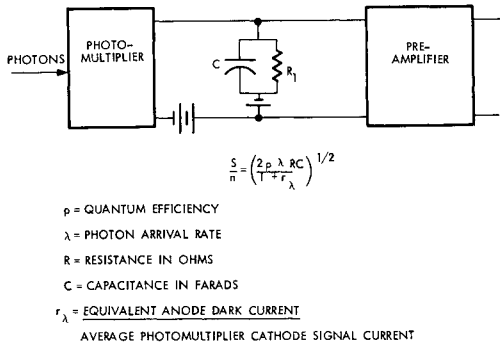

Fig. 7 Idealized photomultiplier output circuit.

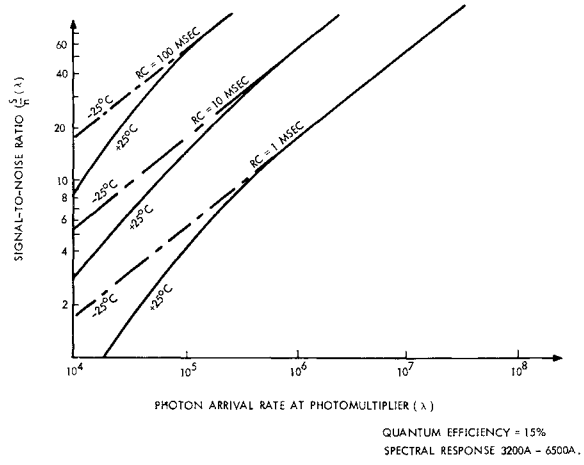

Fig. 8 Signal-to-noise ratio for various photon arrival rates for a typical photomultiplier.

second radical in Eq. (3) becomes $(R/4C)^{1/2}$. The signal-to-noise ratio is by definition $V_s/(\overline{V_n^2})^{1/2}$, both voltages as measured across the resistor R. Therefore,

$$\frac{s}{n} = \frac{iGR}{[2e(i + i_D)G^2 + (4KT/R)]^{1/2}(R/4C)^{1/2}} = \frac{2iG(RC)^{1/2}}{e^{1/2}[2(i + i_D)G^2 + (0.1/R)]^{1/2}} \tag{4}$$

Let

$$i_D/i = r\lambda \qquad i = \rho\lambda e$$

where

ρ = quantum efficiency
λ = photon arrival rate
e = electron charge

With appropriate reduction and simplifying assumptions Eq. (4) becomes

$$\frac{s}{n} = \left(\frac{2\rho\lambda RC}{1 + r_\lambda}\right)^{1/2} \tag{5}$$

It is to be noted that r_λ is a function of photon arrival rate λ and of the temperature. The term r_λ decreases as the temperature decreases. The signal-to-noise ratio is plotted against the photon arrival rate in Fig. 8 at temperatures of 25° and −25°C for a typical photomultiplier tube.[6]

Determination of the signal-to-noise ratio of the error angle voltage as a function of the signal-to-noise ratio of the pulse train from the photomultiplier will be done assuming that the four sequential pulses are sampled instantaneously, although the analog sampling methods require a finite amount of time. The two cases will be considered for image offset which are: 1) image centered at the origin, resulting in a pulse train of four pulses of equal amplitude; 2) image located entirely in one quadrant with 100% reflectivity, resulting in one pulse.

In both cases, the slit jaws are considered to have the coating which reduces the reflectivity adjacent to the slit jaws to 50%. When the image is centered on the slit 50% of the energy falls through the slit and 50% of the remainder is absorbed by the coating on the slit jaws. The division of energy to either side of the slit, giving the Z axis discrimination, reduces the remainder by 50%. Division of the energy to obtain the Y axis discrimination divides each pulse in half giving a further reduction of 50%. Under these conditions, the ratio of the single pulse amplitude to the amplitude of the four equal pulses is 16.

In summary: $16 \times 0.5 \times 0.5 \times 0.5 \times 0.5 = 1$ amplitude of each pulse (case 1). For the purposes of the following signal-to-noise discussion, let S_V denote the full signal voltage corresponding to the case 2 pulse and N_V the rms error sensor noise. For case 2

$$S_V/N_V = (s/n)4\lambda \tag{6}$$

where the signal-to-noise ratio as a function of λ is obtained from Fig. 8 if the equivalent photon arrival rate λ for case 1 is known. In case 1, four pulse amplitudes are processed for one error angle measurement. The rms noise voltage N_V is therefore twice the rms noise amplitude of the four pulses.

For case 1:

$$S_V/N_V = 8(s/n)(\lambda/4) \tag{7}$$

The error angle voltage signal-to-noise ratio S_V/N_V vs the photon arrival rate is plotted in Fig. 9 for acquisition and for the null position. The rms noise error angles $(\overline{Y^2})^{1/2}$ and $(\overline{Z_2})^{1/2}$ are obtained from the transfer characteristics by determining the error angles corresponding to the given rms error angle voltage.

To determine the error angle voltage signal-to-noise ratio for a star of seventh magnitude which is the faintest star for which guidance signal is required, the following parameters have been established[4]: power from a star of seventh magnitude $= 1.04 \times 10^{-11}$ erg/sec/cm^2/Å at 4370 Å; light-gathering efficiency of telescope system $= 2.45 \times 10^3$ cm^2; and efficiency of sensor system $= 7.1 \times 10^{-3}$. Then

$$\text{power at detector} = 1.04 \times 10^{-11} \times 2.45 \times 10^3 \times 7.1 \times 10^3$$

$$= 1.8 \times 10^{-10} \text{ erg/sec/Å}$$

The sensitive range of the detector is from 2900 to 5400 Å, giving a bandwidth of 2500 Å. The energy of a photon at 4000 Å is

$$E = \frac{hc}{\lambda} = \frac{6.623 \times 10^{-27} \times 3 \times 10^8}{4 \times 10^{-7}} = 5 \times 10^{-12}$$

erg/photon

h = Planck's constant, 6.623×10^{-27}
c = velocity of light, 3×10^8 m/sec
λ = wavelength, m

The number of photons per second to be received at the detector is

$$N = \frac{1.8 \times 10^{-10} \times 2.5 \times 10^3}{5 \times 10^{-12}} = 0.9 \times 10^5 \text{ photon/sec}$$

Using this value in Fig. 9, the noise voltage for a seventh-magnitude star will be approximately 50/1 for the sensor when stationary at null. This noise voltage corresponds to a noise angle of 0.012 arc sec as obtained from Fig.5.

The sensor will have the capability of guiding on a given star and discriminating from other stars in the field that are one order of magnitude fainter. Stars that are within one magnitude of the guide star will displace its image from being exactly centered on the slit jaws. The star to be studied will be selected so that no other star within the field of the sensor will be as bright as one magnitude less than the guide star.

To assure reliable operation of the sensor for one year in orbit, redundancy has been used for many of the critical functions. Two complete sensor systems are provided with parallel capability implemented between and within the systems. Two control registers are provided and they are so connected that either one may be used with either system. The series chain from motor to preamplifier may be used with either main amplifier system. The outputs of the sensor systems are connected together to supply the control signal to the spacecraft. Control of the redundancy capability is provided within the Experiment electronics by the redundancy control unit which is operated by digital commands from the ground. These commands are processed by the spacecraft, since the Experiment contains no transmitting or receiving equipment. To prevent interaction between the redundant parts, power is applied only to those units that are to be operated, by means of relays.

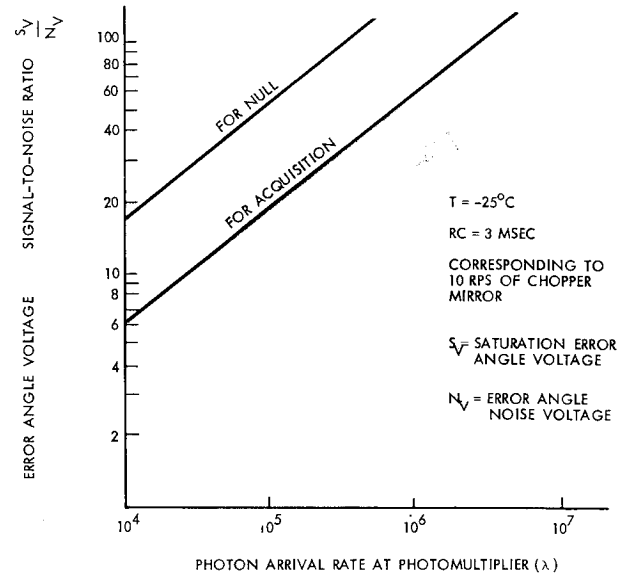

Fig. 9 Sensor signal-to-noise ratio vs photon arrival rate for acquisition and null position.

In determining the probability of successful operation of the sensor, the control registers may be considered nonessential in that the remainder of the equipment will operate and provide control capability but without the ability to program an offset to account for drift or other displacements of the image.

The probability of successful operation of the combined units that make up the sensor system exclusive of the control registers has been computed,[2] considering the several states where failure of one or more elements will not prevent successful system operation. This probability is 0.9387 for successful operation of the sensor for one year in orbit. When the control registers are included in this analysis, the probability becomes 0.9382. It should be emphasized that this is just one of several systems whose operation is necessary to the successful performance of the Princeton Experiment.

References

[1] Arbenz, K. A., "Guidance system—final design plan," Princeton Experiment Program Monthly Rept. 5, Sylvania Electronic Systems (February 1963).

[2] Emero, R., "Reliability analysis—PEP guidance system," Princeton Experiment Program Monthly Rept. 6, Sylvania Electronic Systems (March 1963).

[3] *OAO Spacecraft Handbook* (Grumman Aircraft Engineering Corp., Bethpage, N. Y., September 1961), Secs. 2, 3, and 8.

[4] Rogerson, J. B., "Stellar flux data," private correspondence (February 1963).

[5] Spitzer, L., Jr., "Space telescopes and components," Astron. J. 65, no. 5, 250–252 (June 1960).

[6] "Princeton Experiment Program—design study report," Sylvania Electronic Systems (June 1963).

[7] "Specification for the Princeton Experiment Package," Sylvania Electronic Systems, Specification 01-504000-1 (August 1962).